Hindawi
Shock and Vibration
Volume 2019, Article ID 3096291, 10 pages
https://doi.org/10.1155/2019/3096291

Research Article

Design and Experimental Study on Shock-Absorbing Steel Bar with Limit Function for Bridges

Zhaoguang Li,[1,2] **Ri Gao**,[1] **and Wei Jia**[1]

[1]*Beijing Jiaotong University, Beijing 100044, China*
[2]*Beijing City University, Beijing 101399, China*

Correspondence should be addressed to Zhaoguang Li; 20005385@qq.com

Received 10 July 2019; Accepted 10 September 2019; Published 7 October 2019

Academic Editor: Marcello Vanali

The existing research on shock-absorbing steel bars is only limited to simply supported beam bridge. In order to expand the application of shock-absorbing steel bars to other fields, this paper develops a novel shock-absorbing steel bar with limit function, and it is suitable for continuous beam bridges. The structure and working mechanism of the shock-absorbing steel bar are analyzed. Three sets of specimens of the shock-absorbing steel bar are fabricated and then repeatedly loaded by the designed quasistatic loading device, in order to investigate their seismic performance parameters, including hysteresis curve, skeleton curve, and initial stiffness and equivalent viscous damping ratio. The results show that when the displacement of the specimen exceeds the initial gap, it enters the stage of energy dissipation and has a stable hysteresis curve and good fatigue resistance. Besides, the shock-absorbing device has a high initial stiffness and can provide stable bearing capacity after yielding. The equivalent viscous damping ratio reflects that the designed shock-absorbing steel bar has good energy dissipation capacity.

1. Introduction

Shock-absorbing dampers are usually installed at the connection of the upper and lower structures of a bridge. Using the friction or plastic deformation generated by the dampers, the dampers can dissipate part of the energy transferred to the bridge and reduce the seismic energy withstood by the bridge, thereby protecting the bridge.

Commonly used dampers are classified into speed-dependent dampers and displacement-dependent dampers. For speed-dependent dampers, the energy dissipation capacity is related to speed; that is, the faster the deformation speed, the greater the damping force. For displacement-dependent dampers, they use the hysteretic deformation of the dampers to dissipate energy, and the energy dissipation capacity is related to the displacement generated by the dampers. So, displacement-dependent dampers are a kind of shock-absorbing device that has certain stiffness adjustment capacity and certain energy dissipation capacity and can provide an additional damping ratio for the structure. Among various displacement-dependent dampers, metal damper has received the most attention. At present, researchers have developed many kinds of dampers, e.g., *X*-shaped stiffened steel plate damper [1], triangular stiffened steel plate damper [2], honeycomb steel plate damper [3], grooved steel plate damper [4], *E*-shaped steel damper [5], rod- and bar-type damper [6], and steel cushion [7, 8].

Shock-absorbing steel bar is a shock-absorbing device designed by Gao and Li [9] for reducing the seismic energy transferred to railway bridges using the design principle of "separation of support's functions." It belongs to an isotropic bar-type displacement-dependent damper. Meng et al. [10] comprehensively investigated the performance indexes of strength, stiffness, hysteresis performance, and energy dissipation capacity of integrated shock-absorbing steel bars and analyzed their damping effect in multispan railway simply supported beam bridges. Li et al. [11]

developed a separated shock-absorbing steel bar and studied its working mechanism, performance parameters, and design principles. Liu and Gao [12] developed a steel restrainer bar system on railway bridges and analyzed its hysteresis performance and limit effect. The aforementioned researchers focus on the application of shock-absorbing steel bars to simply supported beam bridges. Therefore, it is necessary to further research the application of shock-absorbing steel bars to continuous beam bridges.

Under the action of strong earthquakes, the seismic forces of the bridge piers of continuous girder bridges are seriously uneven. The piers with fixed supports bear most of the seismic force, resulting in large plastic deformation at the bottom of the piers and further causing the concrete at the bottom of the piers to peel off or even the beam to collapse. By contrast, the piers with movable supports produce larger relative displacements between the pier and the beam, but they do not fully exert their seismic resistance and do not make full use of their surplus strength. In view of this problem, this paper proposes to install a shock-absorbing device on the top of a movable pier. Through the energy dissipation capacity and limit function of the shock-absorbing device, the relative displacement between the pier and the beams of continuous beam bridge is confined, the seismic horizontal force shared by the movable pier is increased, and the seismic force of the fixed pier is reduced, thereby improving the seismic performance of the continuous beam bridge. Based on the aforementioned ideas, this paper proposes a novel shock-absorbing steel bar with limit function and energy dissipation function and systematically investigates the structure design, working mechanism, and hysteretic behavior of the designed shock-absorbing steel bar.

2. Structure and Working Principle of the Shock-Absorbing Steel Bar

2.1. Structure of the Shock-Absorbing Steel Bar. The shock-absorbing device mainly consists of steel cylinders, limited rings, retaining rings, steel bars, bolts and nuts, ring flange, and rubber seals, as shown in Figures 1(a) and 1(b). The steel bar consists of two separated steel bars of identical structure, and the separated steel bar consists of two parts: the bar and the ring flange. The two separated steel bars are connected by the ring flange and bolts and nuts. The limit ring is mounted and fixed inside the preburied steel cylinder, and an initial gap is set between the retaining cylinder and the steel bar. The retaining ring is installed outside the preburied steel cylinder and is in contact with the maximum cross-sectional position of the bar, and a small gap is also set between the two to facilitate the rotation of the steel bar during operation. The rubber seal is used to seal the gap between the retaining ring and the steel bar to prevent debris from entering the interior of the preburied steel cylinder and fill the initial gap between the limited ring and the bar. The partial section of the contact position between the steel bar and the retaining ring and the retaining ring adopts an equal section design. Besides, the section is appropriately widened to ensure the stability of the section of the contact position between the steel bar and the retaining ring, thereby forming stable working performance.

The shock-absorbing device can be divided into two parts according to its function. One part is the limit part consisting of the preburied steel cylinder, the limited ring, the retaining ring, and the bar installed inside the steel cylinder. The other part is the energy dissipation part consisting of the bar outside the steel cylinder, the flange, and bolts and nuts.

The shock-absorbing device has the following characteristics:

(1) The shock-absorbing device has an initial gap, and thus, the normal operation of the bridge structure will not be affected by the shock-absorbing device

(2) The energy dissipation part is designed with equal strength to ensure that when the force on the bar reaches a certain value, the sections of the steel bar can simultaneously yield and enter the plastic stage

(3) The steel bar adopts a circular section, which can provide the same stiffness and damping in any direction and can achieve the functions of limit and shock dissipation in different directions

(4) The upper and lower steel bar of the shock-absorbing device are separated, which is easy to install and replace

2.2. Working Principle of the Shock-Absorbing Steel Bar. The working states of the shock-absorbing device can be divided into two stages. (1) Under the normal operation of the bridge structure, when the relative displacement between the pier and the beam generated by the structure does not exceed the initial gap of the shock-absorbing device, the shock-absorbing device is at the working state of free displacement and does not provide any force on the bridge structure, as shown in Figure 2(a). (2) When the bridge structure is subjected to seismic load and the relative displacement between the pier and the beam exceeds the initial gap, the energy dissipation part enters the working state, and its functions of limit and shock absorption start to work, as shown in Figure 2(b).

Under the normal operation of the bridge, the deformation of the bridge structure generally results from the temperature load, concrete shrinkage and creep load, and horizontal load of the moving vehicles. At this time, the shock-absorbing device is in the first working stage in which the steel bar can be freely displaced. Therefore, the initial gap of the shock-absorbing device is determined by the deformation caused by the normal operating load of the bridge structure.

2.3. Installation of the Shock-Absorbing Steel Bar. Shock-absorbing steel bars are installed between the top of the pier and the bottom of the beam and work together with sliding bearings. The installation schematic is shown in Figure 3. The steel cylinder is embedded in the

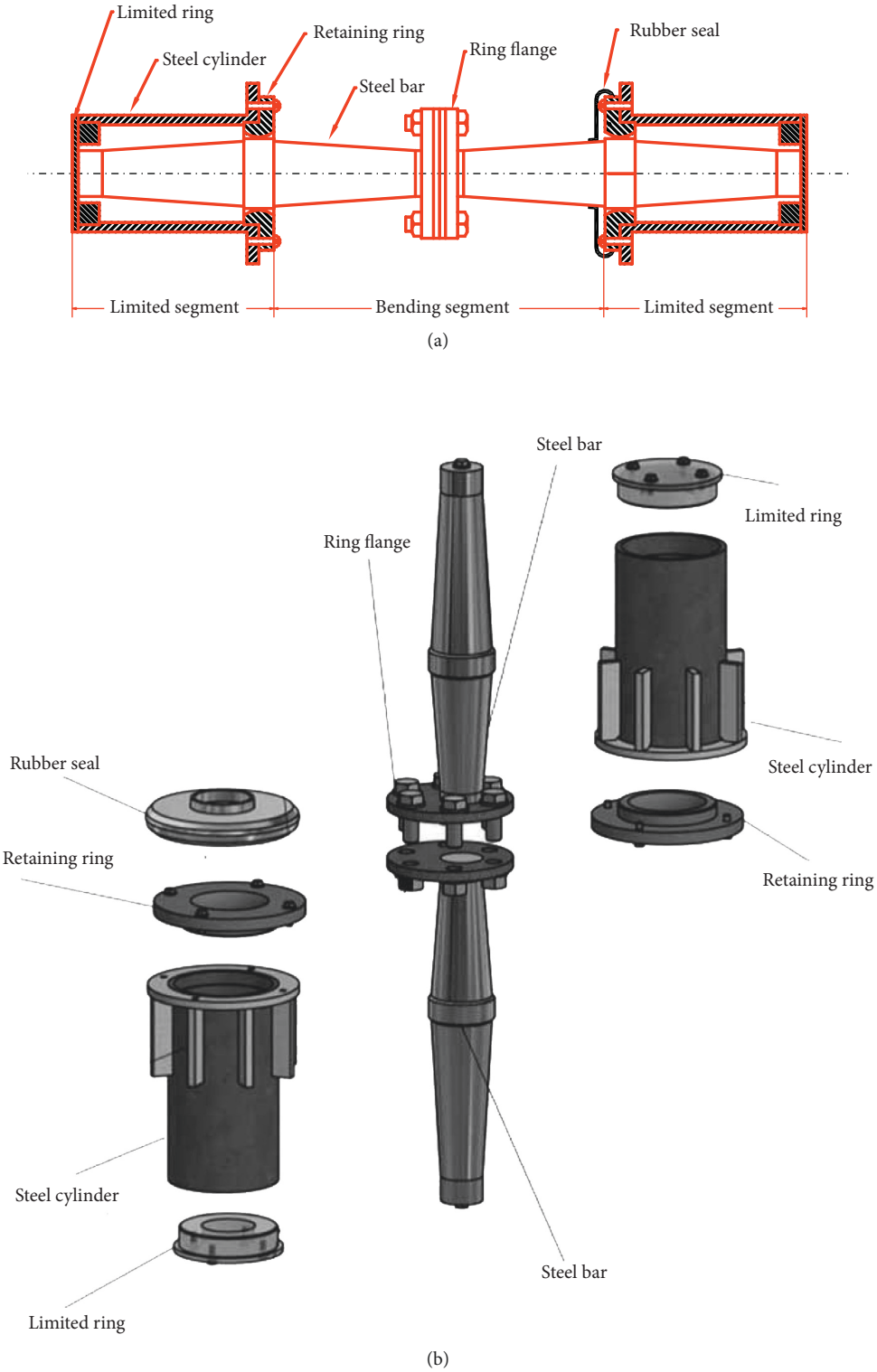

Figure 1: Structure of the developed shock-absorbing device. (a) Details of the device. (b) Disassembly diagram of the device.

concrete. The stiffening ribs can be set outside the steel cylinder to increase the contact area with the concrete and to enhance the imbedding effect of the steel cylinder in the concrete.

Installation of the steel cylinder at the bottom of the beam adopts the preburied method, and steel cylinders are placed at the bottom of beams during beam production. The method of reserved hole can be used to install the

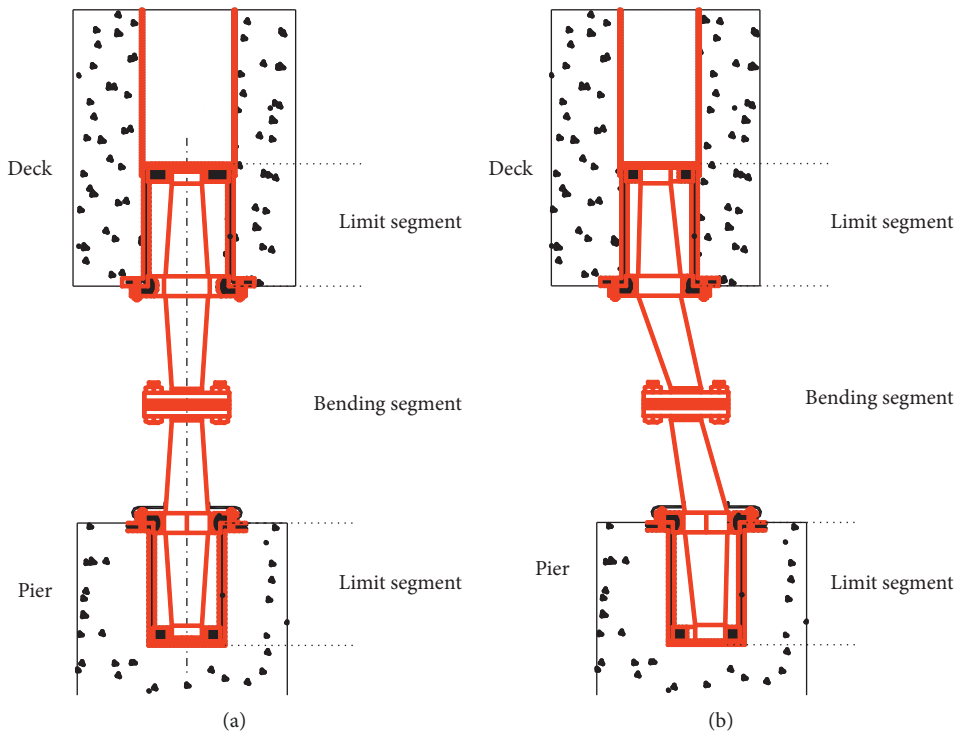

Figure 2: Schematic diagram of the working conditions of the shock-absorbing device. (a) Deformation diagram of the shock-absorbing device with small displacement. (b) Deformation diagram of the shock-absorbing device with large displacement.

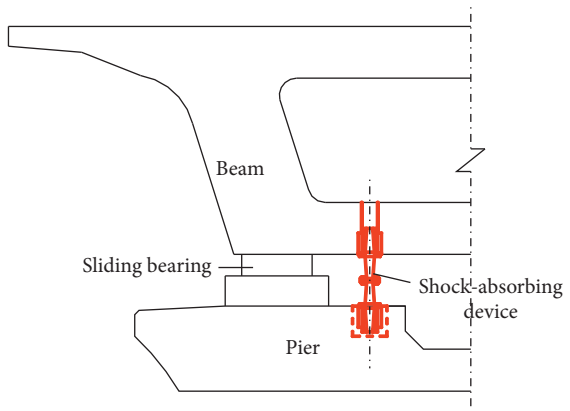

Figure 3: Shock-absorbing steel bar installment.

embedded steel cylinder on the pier top. The embedded location should be accurate.

3. Experimental Setup

3.1. Experimental Design. In the quasistatic test, three sets of 1 : 1 shock-absorbing steel bar specimens were made. The specimens were numbered as 350-1, 350-2, and 350-3. The initial gap of the shock-absorbing device is 30 mm, the designed displacement is 120 mm, the limit displacement is 160 mm, and the limit load is 350 kN. The geometric dimensions of the specimen are shown in Figure 4.

3.2. Experimental Device. The experimental device for the quasistatic test is shown in Figure 5, and the installed device is shown in Figure 6. The experimental device mainly consists of MTS servo actuator, support frame, fixed table, and shear wall. The MTS servo actuator is used to execute the command of the main controller; to control the speed, direction, displacement, and force of the load during the test; and to feedback the information such as force and displacement to the main controller. The MTS servo actuator used in the test has a maximum force of 630 kN and a maximum stroke displacement of 250 mm. The fixed table simulates the situation where the shock-absorbing steel bar is installed on the pier and the beam, so that the working environment of the specimen is close to the actual one. The shear wall provides a fixed position for the MTS servo actuator and withstands the reaction of the actuator.

One end of the MTS servo actuator is fixed to the shear wall by high-strength bolts, and the other end is locked to the slide core by a connecting device. The sliding core is embedded in the slide of the support frame, and the sliding core is fixed with the upper preburied steel cylinder, so that the upper preburied steel cylinder can be synchronously displaced with the sliding core. The lower preburied steel cylinder is embedded in the concrete fixed table, and the steel bar of the shock-absorbing device is installed inside the upper and lower steel cylinders. During the test, the MTS servo actuator provides a cyclic reciprocating displacement load for the sliding core, and the sliding core drives the shock-absorbing device to perform periodic reciprocating motion. The concrete fixed table is fixed with the support frame, and the two did not undergo any displacement during the whole test.

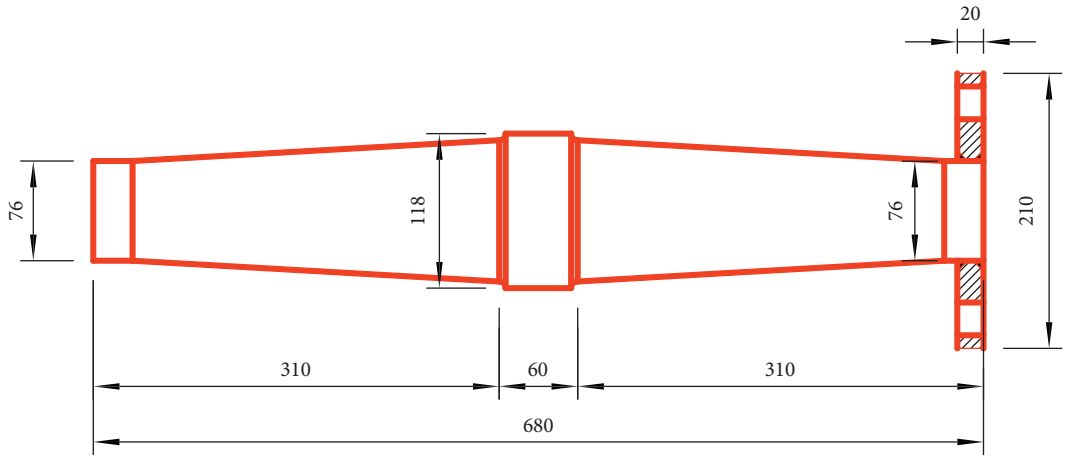

Figure 4: Geometric dimensions of the specimen.

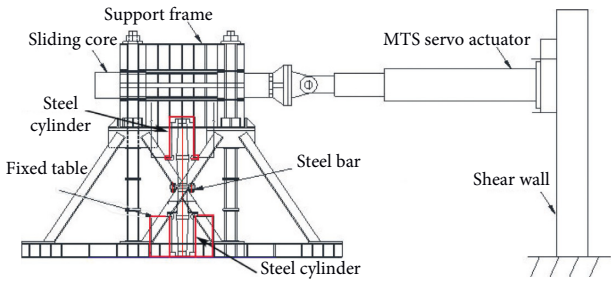

Figure 5: Schematic diagram of the experimental device.

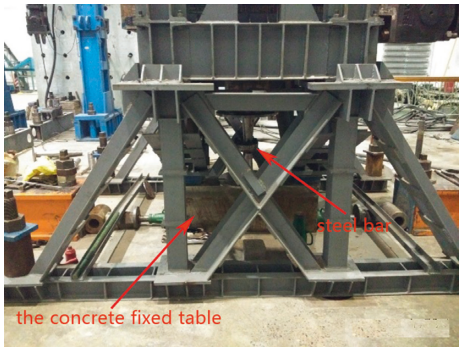

(a)

(b)

Figure 6: Installed experimental device. (a) Test installation completion diagram and (b) MTS 244.41 servo actuator.

3.3. Loading Strategy. In the quasistatic test, the mechanical properties of the specimen are investigated by applying the load in two stages. The first stage is the standard loading test. An equal step-increasing displacement load is applied to the specimens 350-1, 350-2, and 350-3. The loading displacements are 40 mm, 60 mm, 80 mm, 100 mm, 120 mm, 140 mm, and 160 mm, and 3 cycles are executed for each displacement. The second stage is the limit-displacement cyclic loading test where the specimen is repeatedly loaded and unloaded under the limit-displacement load. This stage of test investigates the stability of low cycle fatigue of the specimens. After the standard loading test is completed, the specimen is made to stand for a period of time, and then the limit-displacement load of 160 mm is applied to the specimen for the second stage of test. When the specimen is broken or the bearing capacity is significantly reduced, the second stage of test is stopped.

The loading strategy of the standard loading test is shown in Figure 7. Drift ratio is defined as the ratio of the top displacement to the height of the shock-absorbing steel bar.

4. Experimental Results and Analysis

4.1. Experimental Process and Phenomena. In the quasistatic test, after the three sets of shock-absorbing specimens complete the standard loading test, the surface of the specimen was smooth and crack-free, and all showed good hysteresis performance. After the specimen was allowed to stand for a period of time, a low-cycle fatigue test was performed under a displacement of 160 mm.

The specimen 350-1 was destroyed after 89 cycles, and obvious macroscopic cracks appeared at the surface of the lower steel bar. The maximum bearing capacity of the specimen was significantly reduced, and the test was stopped. The final shape of the specimen is shown in Figure 8.

The specimen 350-2 was destroyed after 73 cycles. The lower steel bar broke, the upper steel bar produced

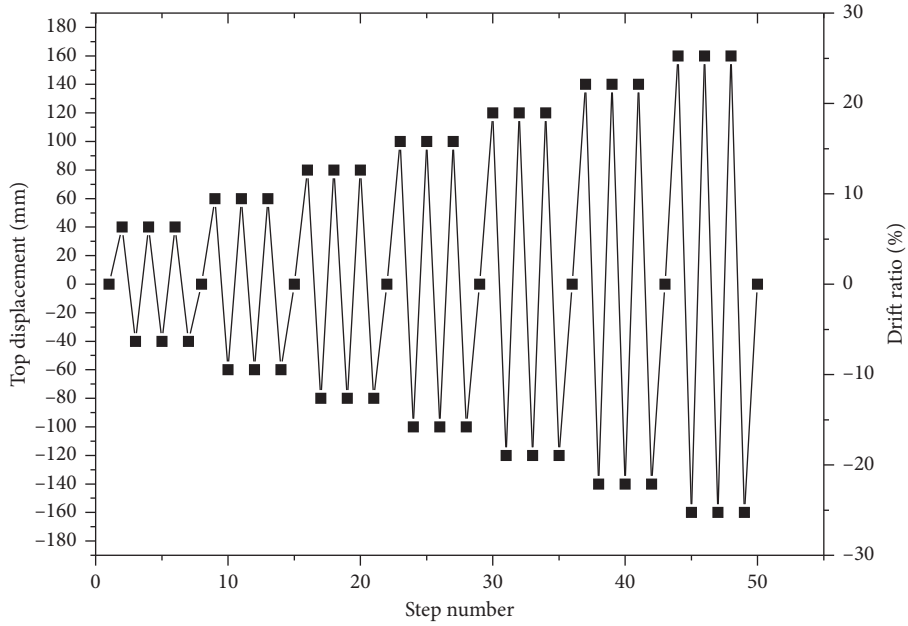

Figure 7: Loading strategy of the standard loading test.

(a) (b)

Figure 8: Failure form of specimen 350-1.

microcracks, and the steel bar showed obvious plastic residual deformation after unloading. The final shape of the specimen is shown in Figure 9.

The specimen 350-3 was destroyed after 89 cycles. The lower steel bar broke, and it was clearly observed from the fracture that the plastic deformation continued to accumulate and ended in fatigue failure. The final shape and fracture of the specimen are shown in Figure 10.

With a maximum displacement capacity of 160 mm, the failure loads of the three specimens are close to each other. The specimen 350-1 is 331 kN, specimen 350-2 is 349 kN, and specimen 350-3 is 348 kN.

The failure phenomena of the three specimens were relatively close, as the fatigue failure all occurred in the energy dissipation part of the shock-absorbing steel bar. This indicated that the specimen had good plastic deformation ability and that the specimen could withstand the ultimate displacement load for more than 70 cycles, showing good resistance to low-cycle fatigue.

4.2. Hysteresis Curve. The hysteresis curves of the three specimens were obtained by the quasistatic test, as shown in Figure 11.

The hysteretic curves of specimen 350-2 and specimen 350-3 basically coincide. The hysteretic curves of specimen 350-1 covers a larger area in the small displacement stage. With increase of displacement, the hysteretic curves of specimen 350-1 are gradually close to those of another two specimens.

However, on the whole, it can be seen from the figure that the hysteresis curves of the three specimens are very close, and each hysteresis curve of the steel bar shows a double-fusiform shape with origin symmetry, and the shape is relatively full. The 3-cycle hysteresis curve is basically consistent under each displacement, showing stable mechanical properties and energy dissipation capacity. When the limit displacement is cyclically loaded, the strength and stiffness of the specimen are stable, and there is no phenomenon of drop-off, which indicates that the specimen has good low-cycle fatigue performance and

(a) (b)

Figure 9: Failure form of specimen 350-2.

(a) (b)

Figure 10: Failure form of specimen 350-3.

can ensure stable performance under multiple cyclic loading.

4.3. Skeleton Curve. The skeleton curve indicates the relationship between the load and the displacement and is used to reflect the initial stiffness, yielding load, yield displacement, and ductility of the structure. It is an important basis for analyzing the elastic-plastic dynamic response of the seismic structure. The skeleton curve of the specimen is obtained by analyzing the corresponding hysteresis curve. Specifically, the maximum point under each displacement of the hysteresis curve of the specimen is sequentially connected, and the obtained envelope is the skeleton curve.

Figure 12 presents the skeleton curves of the three specimens. As can be seen from the figure, the skeleton curve has two distinct turning points. The first turning point represents the transition from the stage of free displacement to the stage of elastic deformation. The second turning point represents the transition from the

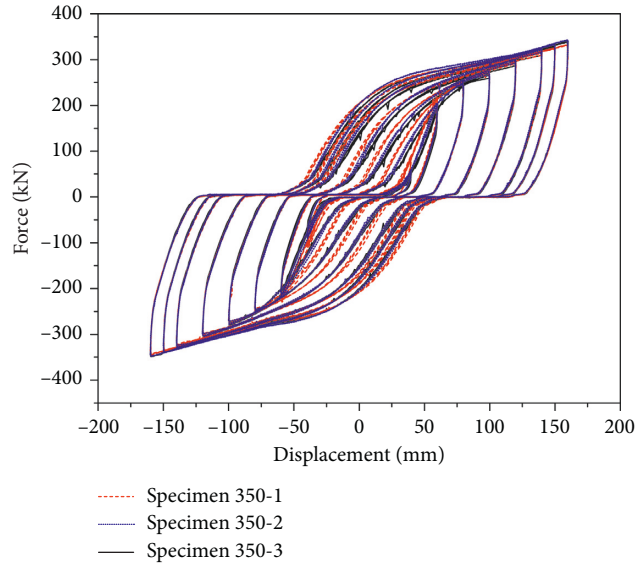

Figure 11: Force-displacement hysteresis curve of the three specimens.

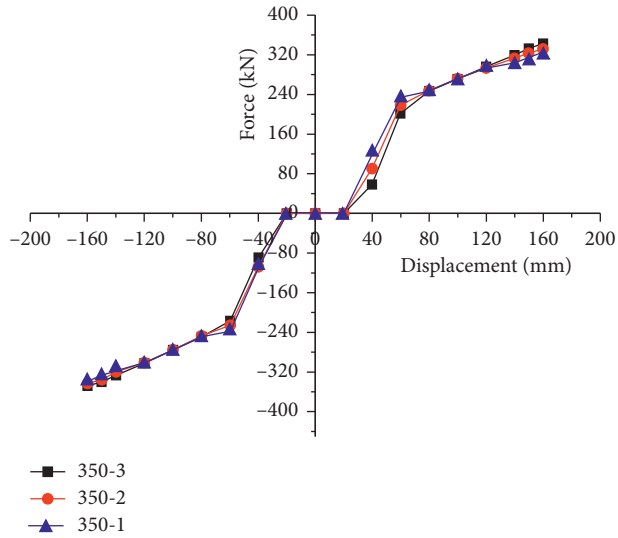

Figure 12: Skeleton curve of the specimens.

stage of elastic deformation to the stage of plastic deformation. The two turning points divide the shape of the skeleton curve into three segments, which are respectively represented as the three working stages of the shock-absorbing device, i.e., the stage of free displacement, the stage of elastic deformation, and the stage of plastic deformation. The shape of the skeleton curve in the positive and negative directions is basically symmetrical with respect to the origin, which represents that the shock-absorbing device has the same mechanical properties under positive and negative loading.

It can also be seen from the figure that the skeleton curves of the specimens 350-1, 350-2, and 350-3 are basically consistent, indicating their stable mechanical properties.

4.4. Main Parameters on Seismic Performance. The main parameters on seismic performance of the shock-absorbing device include initial stiffness K_u, postyield stiffness K_d, yielding load F_y, yielding displacement u_y, limit load F_{max}, limit displacement u_{max}, and initial gap ΔL.

The seismic performance parameters of each specimen can be obtained by fitting the test data of the skeleton curve and hysteresis curve, as listed in Table 1.

The initial stiffness of the steel bar of the device can reach 6 kN/mm or more. The large initial stiffness is beneficial to increasing the limit effect of the device, which helps to avoid the beam dropping caused by the collision between adjacent beams and by the large relative displacement between the pier and the beam under seismic loading. With the increase of displacement, the secant stiffness of the steel bar gradually decreases, and there is a tendency to gradually flatten. This is beneficial for generating the plastic deformation by the steel bar, thereby dissipating the energy transferred into the bridge structure.

The equivalent viscous damping ratio is an important parameter for evaluating the energy dissipation capacity of structural components and reflecting the energy dissipation performance of shock-absorbing devices. In this paper, the equivalent viscous damping ratio ξ_c is still used to measure the energy dissipation performance of the shock-absorbing steel bar in the device. The equivalent viscosity damper ratio ξ_c is calculated by the following equation:

$$\xi_c = \frac{A}{2\pi F u}, \tag{1}$$

where A is the magnitude of the seismic energy dissipated by the hysteresis deformation of the structure and is equal to the area enclosed by the closed hysteresis loop in a cycle; u is the maximum displacement on the hysteresis loop of the structure; F is the load corresponding to the above maximum displacement.

The equivalent viscous damping ratios of the three specimens under each displacement were calculated and plotted, as shown in Figure 13. As the shock-absorbing device is in the elastic state and has no plastic energy dissipation under the displacement of 40 mm, the equivalent viscous damping ratios are calculated from the displacement of 60 mm. The final equivalent viscous damping ratio of the shock-absorbing steel bar is taken as the average of the equivalent viscous damping ratio of each loop of the curve under each displacement.

The equivalent viscous damping ratios of the specimen 350-1,350-2, and 350-3 are 0.278, 0.270, and 0.265, respectively, when the design displacement is 120 mm; they are 0.317, 0.316, and 0.309, respectively, when the limit displacement is 160 mm.

It can be seen from Figure 13 that the equivalent viscous damping ratio of the three specimens has the same trend, and it increases with the increase of the displacement, along with the increasing energy dissipation capacity. The equivalent viscous damping ratio of all the three specimens reach 0.26 under the design displacement of 120 mm and reach 0.3 under the limit displacement of 160 mm, indicating that the designed shock-absorbing device has good performance in deformation and energy dissipation.

Table 1: Mechanical properties of the specimens.

Specimens	Yielding load (kN)	Yielding displacement (mm)	Limit load (kN)	Limit displacement (mm)	Initial stiffness (kN/mm)	Postyield stiffness (kN/mm)
350-1	234	62	336	160	6.32	1.04
350-2	226	62.5	343	160	7.41	1.2
350-3	226	66	338	160	6.64	1.19

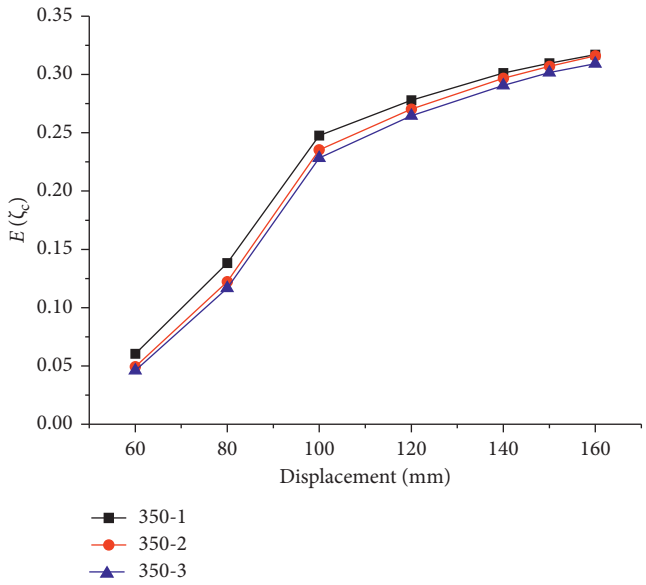

Figure 13: Equivalent viscous damping ratio ξ_c of the shock-absorbing device.

5. Conclusions

In this paper, a shock-absorbing steel bar device with limit function is proposed. Through the quasistatic test on three specimens, the hysteretic behavior and skeleton curve of the shock-absorbing steel bars are investigated, and the seismic performance parameters are analyzed. The main conclusions are summarized as follows:

(1) The shock-absorbing device with limit function is suitable for the seismic design of the nonfixed pier of continuous beam bridge. The working state of the device is divided into two stages. Under the force of normal operating load, the shock-absorbing device is in a working state of free displacement. Under the force of seismic load, the displacement of the shock-absorbing steel bar exceeds the limit displacement and enters the working state of energy dissipation.

(2) The hysteresis curve of the shock-absorbing device is symmetrical double-fusiform, and the hysteresis loops under each displacement are basically consistent, which shows its stable working state. The limit low-cycle fatigue of the shock-absorbing device can endure more than 70 cycles of loading, which shows its good resistance to low-cycle fatigue. The shock-absorbing steel bar has good energy dissipation capacity, and the position of fatigue failure is within the energy dissipation part of the steel bar.

(3) The shock-absorbing device has a high initial stiffness and can provide stable bearing capacity after yielding. The shock-absorbing steel bar has a higher equivalent viscous damping ratio under large displacement, indicating its good energy dissipation capacity.

(4) Further quantification research is required to investigate the damping effect of the shock-absorbing steel bar on continuous girder bridges. The theoretical and experimental methods should be used to further analyze the influence of the shock-absorbing device on the seismic response of the continuous beam bridge so that it can be better applied to practical engineering.

Data Availability

The test data are included within the article and can be made freely available.

Conflicts of Interest

The authors declare that there are no conflicts of interest regarding the publication of this paper.

Acknowledgments

This work was supported by the Project of National High Technology Research and Development Program (Program 863) of China (grant number 2008AA030707).

References

[1] A. S. Whittaker, V. V. Bertero, C. L. Thompson, and L. J. Alonso, "Seismic testing of steel plate energy dissipation devices," *Earthquake Spectra*, vol. 7, no. 4, pp. 563–604, 1991.

[2] K. C. Tai, H. W. Chen, C. P. Hong et al., "Design of steel triangular plate energy absorbers for seismic-resistant construction," *Earthquake Spectra*, vol. 9, no. 3, pp. 505–528, 1993.

[3] Y. Kurokawa, M. Sakamoto, T. Yamada et al., "Seismic design of a tall building with energy dissipation damper for the attenuation of torsional vibration," *The Structural Design of Tall Buildings*, vol. 9, no. 3, pp. 21–32, 1998.

[4] A. Wada, Y.-H. Huang, and M. Iwata, "Passive damping technology for buildings in Japan," *Progress in Structural Engineering and Materials*, vol. 2, no. 3, pp. 335–350, 2000.

[5] P. Tsopelas and M. C. Constantinou, "Study of elastoplastic bridge seismic isolation system," *Journal of Structural Engineering*, vol. 123, no. 4, pp. 489–498, 1997.

[6] C. Donatella, T. Francesco, and B. Paolo, "Seismic protection of Tuy Media Railway viaducts: design and shaking table tests of the seismic devices," in *Proceedings of the 13th World*

Conference on Earthquake Engineering, Vancouver, BC, Canada, August 2004.

[7] H. Ozkaynak, "The effects of special metallic dampers on the seismic behavior of a vulnerable RC frame," *Structural Engineering and Mechanics*, vol. 61, no. 4, pp. 483–496, 2017.

[8] H. Özkaynak, "Earthquake behavior of steel cushion-implemented reinforced concrete frames," *Earthquake Engineering and Engineering Vibration*, vol. 17, no. 2, pp. 385–401, 2018.

[9] C.-g. Li and R. Gao, "Study on the shock absorbing technique of high-speed railway bridges," *Engineering Sciences*, vol. 11, no. 1, pp. 81–86, 2009, in Chinese.

[10] X. Meng, R. Gao, and C. G. Li, "Theoretical and experimental study of hysteretic behavior of shock absorber," *Bridge Construction*, vol. 45, no. 3, pp. 20–25, 2015, in Chinese.

[11] A. L. Li, R. Gao, and C.-g. Li, "Design and experimental study of a novel type of mild steel shock absorber," *Bridge Construction*, vol. 47, no. 1, pp. 23–28, 2017, in Chinese.

[12] C. Liu and R. Gao, "Design method for steel restrainer bars on railway bridges subjected to spatially varying earthquakes," *Engineering Structures*, vol. 159, pp. 198–212, 2018.